https://doi.org/10.5194/egusphere-2025-6106
Preprint. Discussion started: 9 January 2026

Ice Nucleating Particles Variability Across a Megacity

Sebastián Mendoza-Téllez[1,*], Karla Valdés[2], David Ramírez[2], Jan Alexis Cedillo[3], Olivia Rivera-Hernández[4], Fernanda Córdoba[1], Harry Alvarez[5], Javier Miranda[6], Irma Rosas[1], Graciela B. Raga[1], Emma Negrete[1], Leticia Martínez[1], Eva Salinas[1], and Luis A. Ladino[1,*]

[1]Institute for Atmospheric Sciences and Climate Change, Universidad Nacional Autónoma de México, Mexico City, Mexico
[2]División de Ciencias Biológicas y de la Salud, Universidad Autónoma Metropolitana – Xochimilco, Mexico City, Mexico
[3]Escuela Nacional de Ciencias Biológicas, Instituto Politécnico Nacional, Mexico City, Mexico
[4]Dirección de Monitoreo de Calidad del Aire, Secretaría del Medio Ambiente, Ciudad de México, Mexico
[5]Facultad de Ciencias, Universidad Nacional Autónoma de México, Mexico City, Mexico
[6]Instituto de Física, Universidad Nacional Autónoma de México, Mexico City, Mexico

*Corresponding authors: Luis A. Ladino (luis.ladino@atmosfera.unam.mx) and Sebastián Mendoza Téllez (sebastian.mendoza@atmosfera.unam.mx)

Abstract

Megacities are a great source of urban aerosol particles, which can impact cloud formation and the local hydrological cycle. However, the aerosol-cloud interaction in megacities, especially in their different microclimates, is poorly understood. In the present study, the physicochemical and biological properties of urban aerosol particles, along with their ice nucleation abilities as a function of particle size (1.0 μm to 10 μm), were simultaneously characterized at two sites across the Mexico City Metropolitan Area (MCMA). We found apparent differences in the chemical composition, criteria pollutants, and biological content between northern and southern sites in the MCMA, separated by 16 km. The urban MCMA aerosol particles were found to act as ice nucleating particles (INPs), with average concentrations ranging between (0.04 ± 0.04) L^{-1} (at -15°C) and (23 ± 17) L^{-1} (at -30°C). The southern MCMA samples were found to be more efficient INPs, and their ice nucleation abilities correlated positively with $PM_{2.5}$, potassium, and sulfur. On the other hand, the ice nucleation abilities of the measured urban particles at both sites did not correlate with their size nor the presence of biological particles. Overall, the aerosol physicochemical and biological compositions, their sources, and their role in cloud formation at both sites were found to be different. Therefore, the present results demonstrated the presence of two different microclimates within the MCMA. This highlights the importance to consider that aerosol-cloud interactions within a megacity may vary widely, especially when assessing the role of INPs in the development of extreme precipitation events.

https://doi.org/10.5194/egusphere-2025-6106
Preprint. Discussion started: 9 January 2026

1. Introduction

Mexico City and its Metropolitan Area (MCMA) is one of the top megacities worldwide with a population of 21 million inhabitants (Población, 2025). In the 1980s, the MCMA was reported as the most polluted city on Earth (Molina and Molina, 2004); however, since the 1990s, air quality has improved significantly (Lezama and Vargas, 2000). Even so, due to its size and the diverse anthropogenic activities, the MCMA atmospheric processes are complex and far from being completely understood (Molina et al., 2010). Nowadays, poor air quality is one of the major threats for the MCMA inhabitants' health (Riojas-Rodríguez et al., 2014). The impact of the high annual release of particulate matter (PM) (in the order of gigagrams, Gg) on the local climate remains poorly quantified (Castro Romero et al., 2024).

Several studies have provided substantial information to improve our understanding of the physicochemical properties of PM along the MCMA (Aldape et al., 1991; Edgerton et al., 1999; Doran et al., 2007; Querol et al., 2008). For example, Vega et al. (2004) characterized the $PM_{2.5}$ composition of the MCMA, showing that the sulfate (SO_4^{2-}), ammonium (NH_4^+), and total carbon (elemental carbon + organic carbon) average concentrations are higher in the north of the city compared to the southern part (higher by 1.16 µg m^{-3}, 0.8 µg m^{-3}, and 18.49 µg m^{-3}, respectively). This agrees with the data reported by the 2006 MILAGRO (Megacity Initiative: Local And Global Research Observations) project, where a complete evaluation of the regional and global impacts of Mexico's City atmospheric emissions was assessed (Molina et al., 2010).

Several studies found that organic matter has a huge impact on the MCMA's $PM_{2.5}$ composition. Amador-Muñoz et al. (2011) reported a carbon preference index (CPI) larger than 1 on the southwest of the MCMA, suggesting that this part of the city contains more biogenic sources (Amador-Muñoz et al., 2013). Ladino et al. (2018) and Hernández-López et al. (2023) reported clear differences in polycyclic aromatic hydrocarbons (PAHs) between the north and south of the MCMA, with the highest concentrations reported in the northern part of the city. Gasoline-fueled vehicles are likely responsible for local PAHs emissions and could reinforce the microclimate theory, which remarks how local emissions at one megacity's location can promote important local atmospheric processes (Molina and Molina, 2004).

Although the studies above highlight the clear differences in the sources and physicochemical properties of PM in different parts of the MCMA, studies that include simultaneous

https://doi.org/10.5194/egusphere-2025-6106
Preprint. Discussion started: 9 January 2026

measurements at two or more sites are scarce. This is of high importance to understand the microclimates along the MCMA and their relationship with local precipitation events.

Given that most of the precipitation over the tropics comes from ice-containing clouds (Mülmenstädt et al., 2015) and that aerosol particles acting as ice nucleating particles (INPs) are key in mixed-phase cloud (MPC) formation (Rogers and Yau, 1996; Houze, 2014; Kanji et al., 2017), the interplay between aerosol particles and cloud formation in big cities such as the MCMA is urgently needed, especially because extreme precipitation events are predicted to increase with time (Tabari, 2020; Gimeno et al., 2022), causing huge economical and societal impacts in densely populated cities.

The impact of urban particles on ice formation in MPC is well documented (e.g., Hasenkopf et al., 2016; Pereira et al., 2021; Chen et al., 2024). Numerous studies such as that of Zhao et al. (2019), reported that the presence of urban aerosol particles affects the microphysical properties of clouds under moderate convective conditions, decreasing ice crystal number concentration (ICNC) and thus increasing the ice particle effective radius (R_{ei}). Chen et al. (2024) found that urban super-micron traffic-influenced road dust and construction-related dust particles were the primary source of INPs (heat-resistant INPs) at temperatures below -15 ºC in Beijing, China. Nevertheless, given that urban aerosol particles are a complex multicomponent mixture (i.e., biological, dust, black carbon, and biomass burning (BB) particles, among others), they may contain components with contrasting ice nucleation abilities. Although urban centers clearly experience high aerosol concentrations, INP concentrations in megacities do not necessarily increase during heavily polluted periods (e.g., Bi et al., 2019; Cabrera-Segoviano et al., 2022; Chen et al., 2024).

The role of urban particles emitted in the MCMA in ice-cloud formation has been previously evaluated (Knopf et al., 2010; Pereira et al., 2021; Rodríguez-Gómez, 2021; Cabrera-Segoviano et al., 2022; Melchum et al., 2023). The first ice nucleation study in the MCMA was conducted by Knopf et al. (2010) as part of the MILAGRO project. The authors reported that the particles in the northern part of the City are dominated by organics, and can efficiently act as INP under cirrus cloud forming conditions, i.e., relative humidity with respect to ice (RH_{ice}) of ~122 % to 128 % and temperatures of 210 K to 230 K.

https://doi.org/10.5194/egusphere-2025-6106
Preprint. Discussion started: 9 January 2026

Regarding MPC, Pereira et al. (2021) found that the ubiquitous anthropogenic emissions did not have a significant impact on the INP concentrations, with samples collected in rural and urban sites, both in the south of the MCMA. Cabrera-Segoviano et al. (2022) reported an inter-annual variability of INP concentrations (a one order of magnitude difference at temperatures higher than -20 ºC) at southern MCMA between 2018 and 2019, a fact that can be related to the variability in aerosol emissions like re-suspended dust. Rodríguez-Gómez (2021) reported higher INP concentrations in the planetary boundary layer compared to the free troposphere on samples collected in southern MCMA during the BB season, similar to previous studies (Prenni et al., 2012; Jahn et al., 2020; Jahl et al., 2021). Finally, Melchum et al. (2023) evaluated the INP abilities of different airborne microrganisms from tropical places such as MCMA and other sites along Mexico. The authors found that out of the 64 tested microorganisms, only the *Cupriavidus pauculus* (Bproteobacteria) and the *Phaeocystis* sp. (marine phytoplankton) can be relevant to MPC formation (with onset freezing temperatures, T_0 of -11.8 ºC and -16.0 ºC, respectively).

Although PM and INPs have been previously characterized in the MCMA, simultaneous INP measurements at more than one site have never been reported. Therefore, there is poor understanding of the aerosol-cloud interactions within different microclimates of the MCMA. To fill this gap in knowledge, the present study reports the simultaneous characterization (physical, chemical, and biological) of PM as well as their ice nucleating abilities in northern and southern sites within the MCMA. To the best of our knowledge, this is the first time that such comprehensive evaluation of the aerosol-cloud interactions is performed in this megacity.

2. Methods

2.1 Sampling location

Mexico City is a tropical city located at 2240 m a.s.l. (Población, 2025), with a particular topography that influences the accumulation of air pollutants (Molina and Molina, 2004). With a sub-humid climate, the city presents an average annual temperature (between 1950 and 2013) of 15 to 18 ºC (Behzadi et al., 2020). The MCMA experiences three different seasons such as cold-dry: October-February, warm-dry: March-May, and wet season: June-October. The mean annual precipitation within 1950–2013 for Mexico City was reported to vary between 357 mm $year^{-1}$ and 1298 mm $year^{-1}$ (Jáuregui, 2000; Molina et al., 2009; Behzadi et al., 2020; Cabrera-Segoviano et al., 2022).

https://doi.org/10.5194/egusphere-2025-6106
Preprint. Discussion started: 9 January 2026

A short-term field campaign was carried out simultaneously at the north and south of the MCMA during the dry-warm season, i.e., between May 12th and May 20th, 2022. Both sampling sites are located within Mexico City (Fig. 1), and they are ~16 km away from each other.

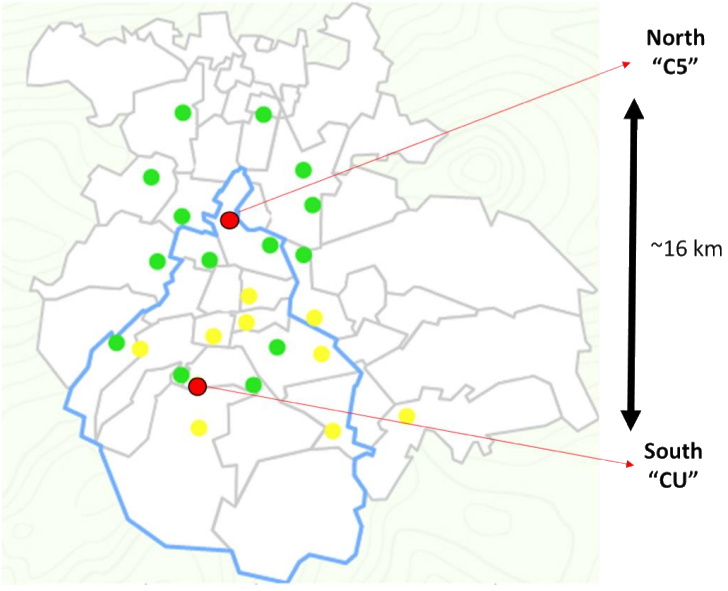

Figure 1. Location of the MCMA showing Mexico City (blue contour) as well as northern and southern sampling sites (red circles). The green and yellow circles represent the Mexico City atmospheric monitoring stations. Modified from https://aire.cdmx.gob.mx/

Sampling at the southern site (CU, 19.3262º N 99.1761º W) took place on the roof of the Institute for Atmospheric Sciences and Climate Change building (approx. 15 m a.g.l.), on the main campus of the Universidad Nacional Autónoma de México (UNAM). Traffic is the primary source of anthropogenic pollution at this site. However, an ecological reserve (237 ha) is located within the main UNAM campus. It can provide biological material to the atmosphere through the native and introduced species of plants, animals, and microorganisms that live in it (Melchum et al., 2023).

On the other hand, the sampling at the northern site (C5, 19.483781º N 99.147312º W) took place on the roof of the Environmental Analysis Laboratory (C5) building (approx. 5 m a.g.l.) of the Mexico City Atmospheric Monitoring System (http://www.aire.cdmx.gob.mx/). The C5 sampling site is subject to a wide range of anthropogenic sources, as it is located in the city's

https://doi.org/10.5194/egusphere-2025-6106
Preprint. Discussion started: 9 January 2026

popularly known "industrial area." Traffic, industrial, and other anthropogenic emissions contribute to high PM atmospheric concentrations at this sampling site (Castro Romero et al., 2024).

Meteorological (T, RH, wind direction, wind speed, solar radiation, and precipitation) and criteria pollutants (CO, O_3, SO_2, NOx, and $PM_{2.5}$) data were recorded on both sites during the sampling campaign (Tables S1 and S2, and Figs. S1 and S2). The campaign dates and sampling hours for the INP abilities are shown in Table 1. Additionally, the ionic composition, elemental composition and culturable microorganisms' identification was obtained using ion chromatography, X-ray fluorescence and different microbiological analysis described in section 2.2.5, all performed on the 24-hour samples collected on May 12th, May 13th, May 16th, May 17th, May 18th, May 19th and May 20th, 2022.

Table 1. Dates, times, and total sampling time for the MOUDI samples used to obtain the INP concentrations. Note that the sampling time was the same at both sites.

Date (month/day/year)	Initial sampling time (local time, h)	Final sampling time (local time, h)	Total sampling time (h)
05-16-22	08:37	12:58	04:21
05-17-22	08:20	12:20	04:00
05-17-22	14:02	18:18	04:16
05-18-22	02:05	06:05	04:00
05-18-22	08:04	12:06	04:02
05-19-22	08:44	12:56	04:12
05-20-22	08:43	12:50	04:07

2.2 Sampling and instrumentation

The simultaneous sampling was performed using, per site, a MiniVol TAS (Tactical Air Sampler; Airmetrics) with a 2.5 μm cut-size inlet that operated at 5 L min^{-1}, an eight stage micro-orifice uniform deposit impactor (MOUDI 100R; MSP) to separate particles as a function

https://doi.org/10.5194/egusphere-2025-6106
Preprint. Discussion started: 9 January 2026

of their aerodynamic diameter (cut sizes of 0.18 μm, 0.32 μm, 0.56 μm, 1.0 μm, 1.8 μm, 3.2 μm, 5.6 μm), and a single-stage BioStage Quick Take 30 cascade impactor for viable particles (SKC Inc. USA) operated at a 28.3 L min^{-1} flow rate. The MiniVol samples were collected on 47 mm Teflon filters (Pall Science) which were used for the ionic and elemental composition analysis. The BioStage impactor was used to collect bacteria and fungi identification (more details are described in section 2.2.5), and the MOUDI samples were used to evaluate the sample's ice nucleating abilities (more details are provided in section 2.2.6).

2.2.1 Meteorological data

Meteorological variables such as temperature, relative humidity, wind direction, wind speed, and solar radiation were obtained from the meteorological stations (Campbell and Davis) of the Red Universitaria de Observatorios Atmosféricos (RUOA) and the Programa de Estaciones Meteorológicas del Bachillerato Universitario (PEMBU) placed in CU and C5, respectively. Also, back trajectories of the air masses arriving in both sampling sites were obtained using the Hybrid Single-Particle Lagrangian Integrated Trajectory (HYSPLIT) model from the National Oceanic and Atmospheric Administration (NOAA) for 72 h at 250 and 500 m a.g.l (Draxler, 2010).

2.2.2 Criteria pollutants

The concentrations of O_3, CO, NOx, and SO_2, were measured with the Teledyne (Sandiego, CA) ultraviolet photometry API Model 400E non-dispersive infrared analyzer, API model 300E, and API model 200E, respectively. The $PM_{2.5}$ was measured with a Thermo Scientific (Franklin, MA) tapered element oscillating microbalance (TEOM) Model 1400A ambient particulate monitor at a flow rate of 3 L min^{-1}.

2.2.3 $PM_{2.5}$ ionic composition

The ionic composition was obtained using a Dionex ICS-1500 ion chromatography (IC) at the Laboratorio de Aerosoles Atmosféricos of the Institute for Atmospheric Sciences and Climate Change, UNAM. For $PM_{2.5}$ aerosol sample extraction, the 47 mm Teflon filters were submerged in 10 mL of deionized water, sonicated for one hour (using an ultrasonic bath at a temperature below 27 °C), and shaken at 350 rpm for six hours (Sartorius CPA225D).

Anion analysis was performed using a Dionex IonPac AS23 column (4 × 250 mm) and a carbonate solution (Na_2CO_3 4.5 mM – $NaHCO_3$ 0.8 mM) as the mobile phase at a flow rate of

https://doi.org/10.5194/egusphere-2025-6106
Preprint. Discussion started: 9 January 2026

1 mL min^{-1}. Three anions were measured using the described setup (NO^{3-}, SO_4^{-2}, and Cl^-). Cation analysis was performed using a Dionex IonPac CS12A column (4 mm × 250 mm) and a methanesulfonic acid (CH_4O_3S 20 mM) with a flow rate of 1 mL min^{-1} as a mobile phase. Five cations were measured using the described setup (Na^+, K^+, NH^{4+}, and Ca^{2+}). The limits of quantification (LOQ) and determination (LOD) were calculated using the linear regression of standards calibration. More details about IC setup and similar methods can be found in Castro Romero et al. (2024).

2.2.4 $PM_{2.5}$ X-ray fluorescence

The elemental composition analysis was performed at the Laboratorio de Aerosoles, Instituto de Física, UNAM following Espinosa et al. (2012). An X-ray fluorescence spectrometer with an Oxford Instruments (Scotts Valley, CA, USA) tube with Rh anode and an Amptek X-123SDD spectrometer (Bedford, MA, USA) was used to obtain the elemental composition of all the particle samples. The instrument was operated at 50 kV and a current of 750 μA, irradiating for 900 s per spectrum. More details of instrument calibration can be found at (Espinosa et al., 2012). The chemical composition was quantified using the methodology reported by Espinosa et al. (2010). The percentage fraction for each element was determined by using the relationship between the analyzed element concentration and the total mass concentration.

2.2.5 Airborne culturable microorganisms' collection and identification

For the microorganism's identification (bacteria and fungi), petri dishes (100 mm × 10 mm) with three different media were used to impact, collect, and grow the microorganisms using the BioStage impactor: trypto-casein soy agar (TSA, BD, Bioxon) supplemented with 100 mg L^{-1} of cycloheximide (Sigma-Aldrich) (to prevent growth fungal propagules) for mesophilic cultivable bacteria (MCB), Reasoner's 2A (R2A, Condalab) for slow-growing species of MCB, and malt extract agar (MEA, BD Bioxon) for cultivable fungal propagules. The sampling time on the BioStage impactor was set to 5 min.

The concentrations of cultivable bacteria were reported as Colony Forming Units per m^3 of air (CFU m^{-3}). The following procedure was applied as described in Melchum et al. (2023). The TSA, R2A, and MEA were cultured at 37 ºC, 35 ºC, and 25 ºC, respectively. After 48 h (for TSA bacteria) and 72 h (for R2A bacteria and fungi), the CFU were quantified, and the Petri dishes were sealed with parafilm and stored at 4 ºC for further analysis. Representative bacterial

https://doi.org/10.5194/egusphere-2025-6106
Preprint. Discussion started: 9 January 2026

colonies were randomly selected and purified by several reseedings in TSA. Gram staining was performed to classify the bacteria as Gram-positive or Gram-negative by microscopic observation (100×) of the preparations. Isolated bacteria confirmation of identity was performed by mass spectroscopy, using the Microflex MALDI214 TOF MS® (Bruker Daltonics, Bremen, Germany). The identification of fungal species was carried out at the genus level using taxonomic keys based on macroscopic colony characteristics and spore microscopic examination (60×) (Rodriguez-Gomez et al., 2020; Melchum et al., 2023).

2.2.6 Ice nucleation experiments

The ice nucleating abilities of the collected aerosol particles were tested using a UNAM-Micro-orifice Uniform Deposit Impactor-Droplet Freezing Technique (UNAM-MOUDI-DFT), described in Córdoba et al. (2021) with its main features shown in Fig. S3.

Aerosol particles were collected on hydrophobic glass coverslips as substrates at each MOUDI stage (flow rate of 30.0 L min^{-1}). After sampling, every substrate was stored in sealed, sterilized Petri dishes at 4 °C until its analysis.

Each glass coverslip was analyzed using the UNAM-MOUDI-DFT to simulate the immersion freezing mode between 0 °C and -40 °C. For the INP experiments, the glass coverslips were placed on a sample holder inside the cold cell with the sample holder at the top of two blocks for a sample temperature control: a heating block (copper-made block with two heating resistances, 100 W and 120 V) and a cooling block (cooled by refrigerator circulator, PRO-RP1090, LAUDA), with the cold block at the bottom. To induce droplet formation, humid air, carried by nitrogen (grade 4.8, INFRA), is directed toward the sample holder at 0 °C. Once approx. 30-40 droplets of ca. 170 μm radius are formed, and a dry airstream is introduced into the cold cell to shrink the droplets, aiming to minimize contact between them. Finally, the cold cell was isolated, and a temperature ramp from 0 °C to -40 °C (at a cooling rate of 10 °C min^{-1}) was run until the freezing of each drop was observed. The entire process was recorded with a video camera (MC500-W, JVLAB) attached to an optical microscope (Axiolab Zeiss, Germany) with a 5×/0.12 magnification objective, the microscope objective being coupled to the sample holder via a glass coverslip at the top of the cold cell.

https://doi.org/10.5194/egusphere-2025-6106
Preprint. Discussion started: 9 January 2026

From the recorded video, it is possible to determine the freezing temperature for each droplet, which allows calculation of the frozen fraction (F_{ice}) and the INP number concentration as a function of temperature ([INP(T)], L^{-1}). F_{ice} was calculated using Equation 1:

$$F_{ice} = \frac{N_{ice}}{N_{ice} + N_{dropplets}} \quad (1)$$

where N_{ice} and $N_{droplets}$ are the number of frozen droplets (dimensionless) and the number of unfrozen droplets (dimensionless), respectively (Kanji et al., 2017).

The [INP(T)] was calculated using Equation 2 (Mason et al., 2015; Córdoba et al., 2021):

$$[INP(T)] = -ln\left(\frac{N_u(T)}{N_0}\right) \cdot \left(\frac{A_{deposit}}{A_{DFT}V}\right) \cdot N_0 \cdot f_{ne} \cdot f_{nu,0.25-0.10\,mm} \cdot f_{nu,1\,mm} \quad (2)$$

where $N_u(T)$ is the number of unfrozen droplets at T (ºC), N_0 is the total number of droplets (dimensionless), $A_{deposit}$ is the total area of the aerosol particles deposited on the hydrophobic glass coverslip (cm^2), A_{DFT} is the area of the sample analyzed by the DFT (cm^2), V is the volume of air through the MOUDI (L), f_{ne} is a correction factor to account for the uncertainty associated with the number of nucleation events in each experiment (dimensionless), and f_{nu} is a correction factor to account for changes in particle concentration across each MOUDI sample (dimensionless). Additionally, this equation accounts for the possibility that multiple particles may be present within a droplet (Vali, 1996), the correction for the total area covered by particles deposited on the MOUDI coverslips, and corrections for inhomogeneities in particle deposition. More details of Equation 2 and the applied corrections can be found in Mason et al. (2015).

2.2.7 Data analysis

The STATISTICA® 12 software (StatSoft, TIBCO Software Inc., USA) was employed to evaluate basic statistics and cluster analysis of data from the different analysis described in section 2.2. With the main objective of identifying associations among chemical species and their possible sources, a cluster analysis using Ward's method of amalgamation and Pearson correlation coefficients was carried out to construct dendrograms for both sampling sites.

https://doi.org/10.5194/egusphere-2025-6106
Preprint. Discussion started: 9 January 2026

3. Results and Discussion

3.1 Frozen fraction and INP concentration variability

Following the procedure described in section 2.2.6, the frozen fraction and the INP concentrations were obtained for each sample from May 16th to 20th. Figure S4 shows the frozen fraction as a function of particle size (aerodynamic diameters of 1.0 μm to 10 μm) for the northern and the southern sampling sites. This size range was selected considering that super-micron particles contribute more than 70 % to the total INP population (e.g., Mason et al., 2016; Córdoba et al., 2021). Aerosol particles collected in the present study were able to nucleate ice at temperatures warmer than those required to freeze supercooled liquid drops (i.e., homogeneous freezing, black line).

For a more quantitative comparison of the ice nucleating abilities of northern and southern samples, the average onset freezing temperatures (T_0) and the average temperatures at which 50 % of the droplets freeze (T_{50}) for each sample were calculated as shown in Fig. 2. The highest average T_0 difference between the northern and southern samples was registered on May 20th, with T_0 values of (-21.1 ± 3.1) ºC and (-17.3 ± 3.4) ºC for C5 and CU, respectively. Additionally, the highest and lowest T_{50} values were recorded on May 20th at CU (-19.8 ± 3.6) ºC and on May 19th at C5 (-26.5 ± 4.4) ºC. The warmest T_0 and T_{50} values reported in this work are slightly higher than those reported by Knopf et al. (2010), Rodríguez-Gómez (2021), Cabrera-Segoviano et al. (2022), and Pereira et al. (2021).

https://doi.org/10.5194/egusphere-2025-6106
Preprint. Discussion started: 9 January 2026

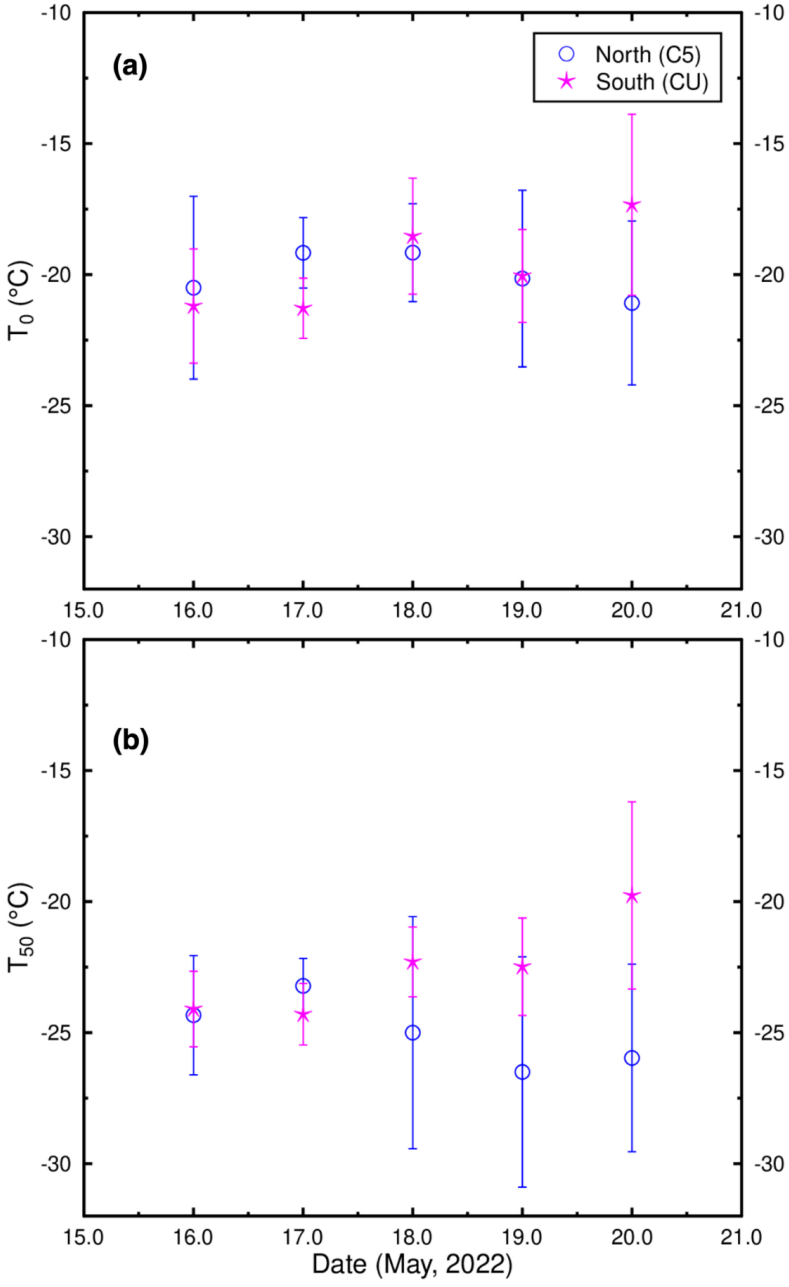

Figure 2. **(a)** Average onset freezing temperatures (T_0) and **(b)** average median freezing temperatures (T_{50}) for samples collected at the north (C5, blue circles) and south (CU, magenta stars) of Mexico City between May 16th and May 20th.

https://doi.org/10.5194/egusphere-2025-6106
Preprint. Discussion started: 9 January 2026

The total INP concentrations at both sites are shown in Fig. 3. Although the INP concentrations measured at both sites were comparable, the exemption was the May 20th sample, were notable higher and statistically significant INP concentrations were measured in the southern site between -12 °C and -22 °C. Figure 3 also indicates that the INP concentrations from the present study agree well with those reported by Cabrera-Segoviano et al. (2022) for Mexico City and by Chen et al. (2024) for Beijing (between -13 °C and -20 °C).

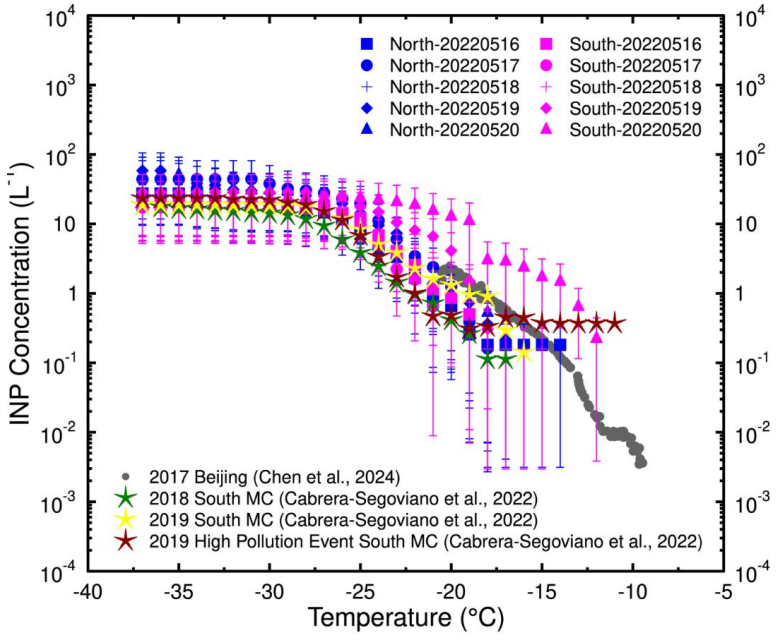

Figure 3. May 16th, 17th, 18th, 19th and 20th INP concentrations for the northern and southern particles as a function of temperature. The colored stars and the gray dots represent the INP concentration values reported for Mexico City (Cabrera-Segoviano et al., 2022) and Beijing (Chen et al., 2024), respectively.

To better assess the differences in the INP concentration across the two microclimates within the MCMA, the average accumulated INP concentrations for both sites at four different temperatures (-15 ºC, -20 ºC, -25 ºC, and -30 ºC) were calculated, as shown in Fig. 4. INP concentrations at both sampling sites are comparable at lower temperatures (i.e., -25 ºC and -30 ºC), while at higher temperatures (i.e., -20 ºC and -15 ºC), the southern samples are higher. At -15 °C, a clear difference of 0.34 L^{-1} can be observed between both sites (C5 (0.04 ± 0.04) L^{-1} and CU (0.38 ± 0.31) L^{-1}). Similar to the data shown in Fig. 3, the INP concentrations

https://doi.org/10.5194/egusphere-2025-6106
Preprint. Discussion started: 9 January 2026

measured in the present study agree with the concentrations reported for southeastern (Rodríguez-Gómez, 2021) and southern sites (Cabrera-Segoviano et al., 2022) of the MCMA.

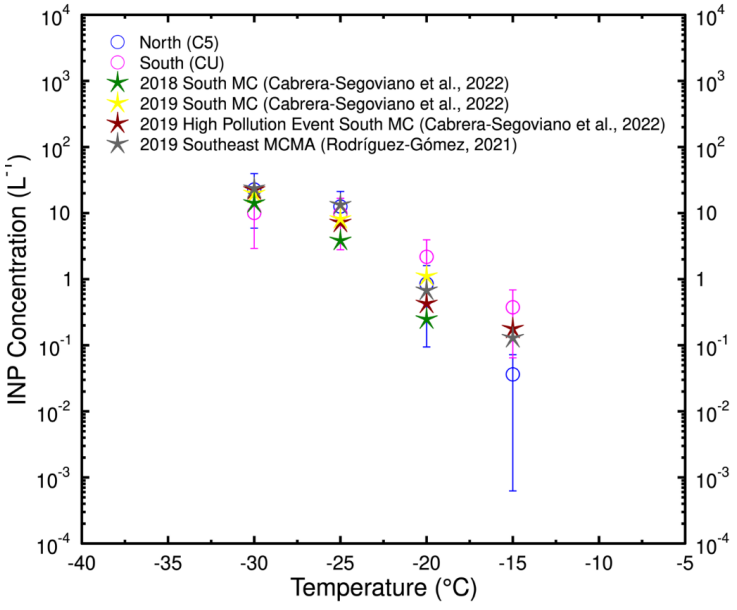

Figure 4. Average INP concentration for the northern (C5) and southern (CU) sites as a function of temperature. While the magenta and blue open circles refer to the present study data, the stars represent the INP concentration values for CU in May 2018 (green), May 2019 (yellow), and May 2019 (red) during a high air pollution episode (Cabrera-Segoviano et al., 2022). The gray stars represent the INP concentration values for the southeast part of the MCMA collected in May 2019 (Rodríguez-Gómez, 2021).

The impact of particle size on the frozen fraction at both sampling sites does not show a clear trend (Fig. S4). Likewise, Figure 5 shows that the INP concentration measured on the urban particles from the MCMA is not clearly size-dependent. In theory, particle size and INP efficiency are related. This relationship is attributed to surface active sites, as larger particles contain a higher concentration of active sites. (Vali, 1996; Hoose and Möhler, 2012; Kanji et al., 2017); nevertheless, this assumption may not work on highly complex samples such as the MCMA urban particles. Different physical and chemical atmospheric processes can modify the INP surface; therefore, active sites can be deactivated in various ways through particle coating and/or aging (Cziczo et al., 2009). Thus, we hypothesize that the complexity in the physicochemical properties of urban particles, may have masked the role of particle size on their ice nucleating abilities.

https://doi.org/10.5194/egusphere-2025-6106
Preprint. Discussion started: 9 January 2026

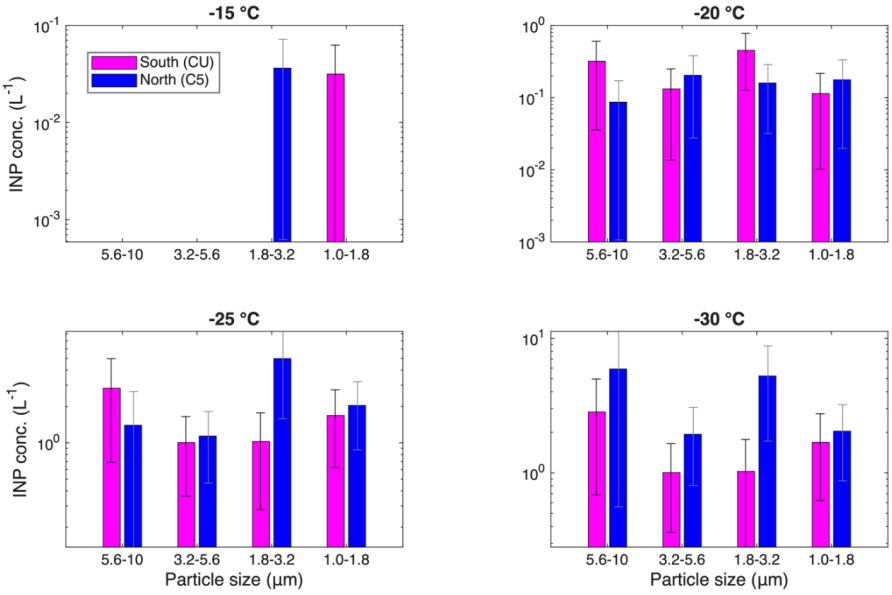

Figure 5. INP average concentration as a function of particle size at -15 °C, -20 °C, -25 °C, and -30 °C, for southern (CU, magenta) and northern (C5, blue) MCMA.

3.2 Ice nucleating activity vs. criteria pollutants and chemical composition

Time series of five criteria pollutant concentrations at both sites are shown in Fig. S2. $PM_{2.5}$ concentration was found to be comparable at both sites, with a slight increase along the last part of the campaign. The maximum difference in $PM_{2.5}$ concentration between both sites was 6.60 µg m^{-3}. Although high hourly values of $PM_{2.5}$ were measured (in the order of ~60 µg m^{-3}), they cannot be considered as *high pollution episodes* as was the case described in Cabrera-Segoviano et al. (2022) where $PM_{2.5}$ concentrations above 80 µg m^{-3} were measured (Carabali et al., 2021). Similar to previous studies performed within the MCMA, CO, SO_2, and NOx concentrations were higher at the northern site, with 0.6 ppm, 14 ppm, and 60 ppm maximum differences between the northern and southern sites for CO, SO_2, and NO_x, respectively (Fig. S2). This behavior is related to local emissions, such as gasoline-fueled vehicular emissions and industrial activity (Vega et al., 2004; Castro et al., 2024). Additionally, meteorological data (Tables S1 and S2, and Fig. S1) support the microclimate theory within the MCMA, showing clear differences in the measured variables between both sites.

O_3 concentrations were higher at the southern site (i.e., a 30 ppm maximum difference between both sites). Local emissions from vegetation cover prevalent in southern MCMA, such as

https://doi.org/10.5194/egusphere-2025-6106
Preprint. Discussion started: 9 January 2026

volatile organic compounds (VOCs), together with local NOx emissions and transport can explain the O_3 behavior. It is well known that VOCs may participate in O_3 production by photochemistry and lead to increased concentrations (Pinto et al., 2010; Amador-Muñoz et al., 2016). Therefore, the southern site is likely enriched in biogenic secondary organic aerosols (SOA) compared to the northern site (Aiken et al., 2009; Cooke et al., 2024). Wang et al. (2012) showed that different types of SOA could act as INPs via immersion freezing with potential to impact MPC formation.

The INP concentrations shown in Figs. 3 and 4 were comparable at colder temperatures, with a slightly higher concentration at the southern site observed on the last sampling day at warm temperatures. Given that a slight increase in $PM_{2.5}$ concentration was also observed on May 20^{th} at the southern site (Fig. S2), there may be a small relationship between INP concentration at warm temperatures and $PM_{2.5}$. Figure 6 shows the calculated Pearson determination coefficients between the measured criteria pollutants and the particle composition with T_0, T_{50} and INP concentration at -20 °C, -25 °C, and -30 °C for both sampling sites. High coefficients were found between $PM_{2.5}$ and T_0, $T_{50,}$ and INP concentrations at -20 °C, especially at the southern site. The relationship between $PM_{2.5}$ and INP concentrations was previously evaluated (Chen et al., 2018; Bi et al., 2019; Córdoba et al., 2021; Cabrera-Segoviano et al., 2022), with contrasting results.

The potential relationship between the ice nucleation abilities of the analyzed urban particles and the other measured variables was assessed. For gaseous criteria pollutants, the southern INPs (T_0, T_{50}, and INP Conc. at -20 °C) positively correlated with O_3 and NOx concentration (Fig. 6). On the other hand, the northern INPs (T_0, T_{50}, and INP Conc. at -20 °C) only correlated with SO_2. Therefore, the importance of the different criteria pollutants on the ice nucleating abilities of the urban particles differs with respect to the microclimate.

https://doi.org/10.5194/egusphere-2025-6106
Preprint. Discussion started: 9 January 2026

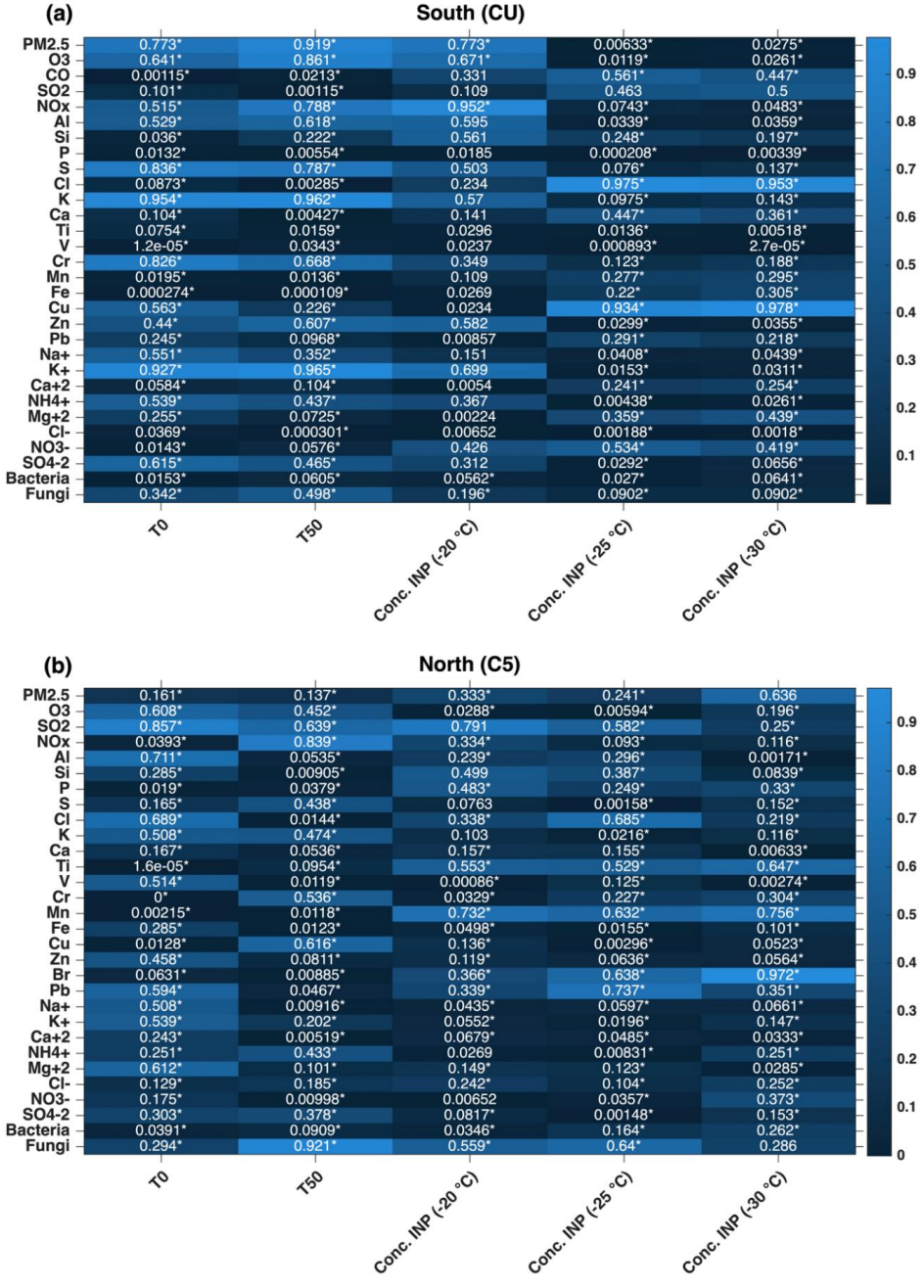

Figure 6. Heat map with the Pearson determination coefficients for the relationships between the ice nucleation abilities of the urban particles and their composition as well as ambient criteria pollutants for **(a)** southern (CU) site and **(b)** northern (C5) site of the MCMA. The statistically significant coefficients are marked with an asterisk.

https://doi.org/10.5194/egusphere-2025-6106
Preprint. Discussion started: 9 January 2026

The analysis of the elemental composition indicates that the concentration of 12 of the 16 analyzed elements (i.e., Si, P, S, Cl, K, Ca, Ti, V, Fe, Cu, Zn, and Br) was higher at the northern site as shown in Fig. 7. The maximum measured concentrations were reported for Al and Si, an indication of the presence of aluminum silicates from resuspended dust, as previously reported (Querol et al., 2019; Córdoba et al., 2021). Pb was present at both sampling sites with a maximum concentration of 0.13 μg m^{-3} and 0.08 μg m^{-3} for CU and C5, respectively. The Pb sources are typically linked with local industrial activities and the usage of low quality fuels (Moreno et al., 2008; Hernández-López et al., 2020). The World Health Organization (WHO) recommends an annual average airborne Pb concentration of 0.5 μg m^{-3} as part of its Global Air Quality Guidelines; therefore, the values reported in this work did not exceed this limit.

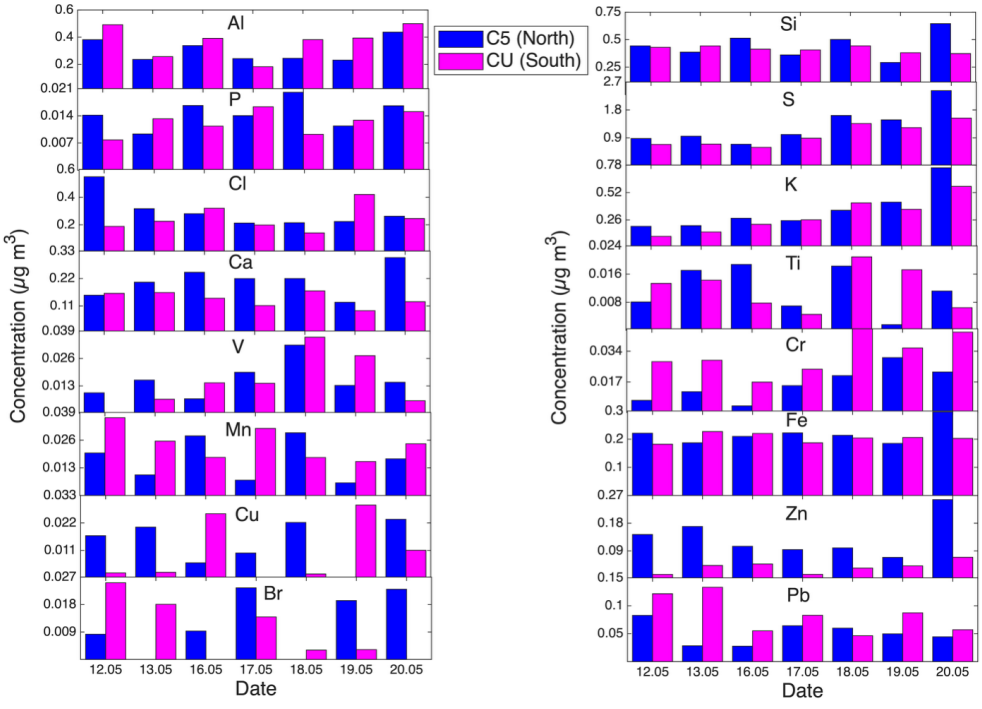

Figure 7. Concentration of the different individual elements analyzed by XRF on $PM_{2.5}$ at the northern (C5, blue) and southern (CU, magenta) sites.

The maximum S concentration (i.e., 2.42 μg m^{-3}) observed in C5 is lower than the values reported in previous studies (3.24 μg m^{-3}, Castro et al., 2024; 3.38 μg m^{-3}, IMADA, 1997; 5.10 μg m^{-3}, Vega et al., 2004), likely related to differences in the sampling month, but higher than the highest S concentration reported in CU (i.e., 1.54 μg m^{-3}). S and K are markers of high-pollution events in megacities, typically linked with industrial activity, gasoline combustion,

https://doi.org/10.5194/egusphere-2025-6106
Preprint. Discussion started: 9 January 2026

and BB emissions (Ríos and Raga, 2018; Raga et al., 2021). In this study, a rise in S and K concentrations during the last sampling day (i.e., May 20th) is clearly observed and could be attributed to local and regional BB. Figure 6 shows that the S and K concentrations positively correlated with T_0, T_{50}, and INP Conc. (-20 °C) at the southern site. This could imply a relationship between the INP behavior and the presence of BB particles, a relationship shown elsewhere (Wei et al., 2019), including Mexico City (Cabrera-Segoviano et al., 2022).

To further explore the importance of aerosol composition and its relationship with the INPs at both sampling sites, the ion composition was analyzed. Figure S5 reinforces the notorious differences in the urban particles' chemical composition between the two microclimates. The five analyzed cations (Na^+, K^+, Ca^{2+}, NH_4^+, and Mg^{2+}) and the three analyzed anions (Cl^-, NO_3, and SO_4^{2-}) showed higher concentrations at the northern site. The relationships among SO_4^{2-}, NO_3^-, and NH_4^+ at both sampling sites are shown in Tables S3 and S4. The strong observed correlation suggests the presence of $(NH_4)_2SO_4$ and NH_4NO_3 at both sites, two compounds produced by photochemical reactions driven by emissions from gasoline and diesel (Vega et al., 2004; Hernández-López et al., 2020; Castro Romero et al., 2024). Correlations are stronger at the northern site, indicating a higher probability of photochemical products mentioned before and consequently, more probability of VOCs and anthropogenic SOA (Hallquist et al., 2009).

Although most of the analyzed ions showed a low correlation with the INP parameters at both sampling sites (Fig. 6), K+ values showed strong Pearson coefficients at the southern site with T_0, T_{50}, and INP Conc. (-20 °C) values, reinforcing the influence of BB emissions on INP behavior at the southern microclimate. Figure S6 summarizes the HYSPLIT backward trajectories ran for May 2022. This, in addition to NASA FIRMS real-time active fire locations for May 16th to 20th showed in Fig. S7, suggests that besides local sources, the regional transport of BB particles can be important for the ice-nucleation abilities of the MCMA urban particles, especially at the southern site. Figure S6 also suggests that the air masses arriving at the northern site at noon and midnight, at 250 m and 500 m AGL, were not transported over the southern site, and vice versa.

To evaluate potential sources of the measured urban aerosol particles, a cluster analysis was applied using all the chemical species to generate a dendrogram for each sampling site. The dendrogram for the southern site (Fig. S8) presents three groups: the orange cluster with anthropogenic oxidized and non-oxidized species and a contribution of BB regional emissions;

https://doi.org/10.5194/egusphere-2025-6106
Preprint. Discussion started: 9 January 2026

the blue cluster with geogenic oxidized and non-oxidized species; and the green cluster with resuspended soil originated from rural areas with geogenic species and some anthropogenic contributions. Likewise, the dendrogram for the northern site (Fig. S9) also shows three groups: the orange cluster, which corresponds to anthropogenic oxidized and non-oxidized species; the blue cluster, containing mostly anthropogenic oxidized species from fossil fuels; and the green cluster with oxidized and non-oxidized resuspended soils. This cluster analysis highlights the effect of land use and BB on the chemical composition of the urban particles at these two microclimates of the MCMA.

3.3 Ice nucleating activity vs. culturable microorganisms

To assess the presence of biological particles at both sampling sites, the concentrations of culturable bacteria and fungi were measured in parallel to the INPs. Significant daily variations in bacteria and fungi concentrations at both sampling sites were observed, as shown in Fig. 8. The measured CFU m^{-3} follow the same pattern at both sites. The average concentrations of bacteria and fungi at the northern site were 2774 CFU m^{-3} and 433 CFU m^{-3}, respectively; at the southern site, the average concentrations of bacteria and fungi were 3882 CFU m^{-3} and 509 CFU m^{-3}, respectively. The average bacteria concentrations reported in this study are higher than those reported for Yucatán, México (i.e., 69 CFU m^{-3}) (Rodriguez-Gomez et al., 2020), Tijuana, México (i.e., 340 CFU m^{-3}) (Hurtado et al., 2014), northwestern Amazon, Colombia (i.e., 228 CFU m^{-3}) (Russy-Velandia et al., 2025), and Qingdao, China (i.e., 83 CFU m^{-3}) (Li et al., 2011). In contrast, the average fungi concentrations reported in this work are lower than those reported for Yucatán, México (i.e., 1018 CFU m^{-3}) (Rodriguez-Gómez et al., 2020), and are consistent with the results reported for northwestern Amazon, Colombia (i.e., 642 CFU m^{-3}) (Russy-Velandia et al., 2025) and Qingdao, China (i.e., ~300 CFU m^{-3}) (Li et al., 2011). Consistent with the aforementioned studies, the Gram staining analysis indicated that 57 % of the culturable bacteria were Gram positive.

https://doi.org/10.5194/egusphere-2025-6106
Preprint. Discussion started: 9 January 2026

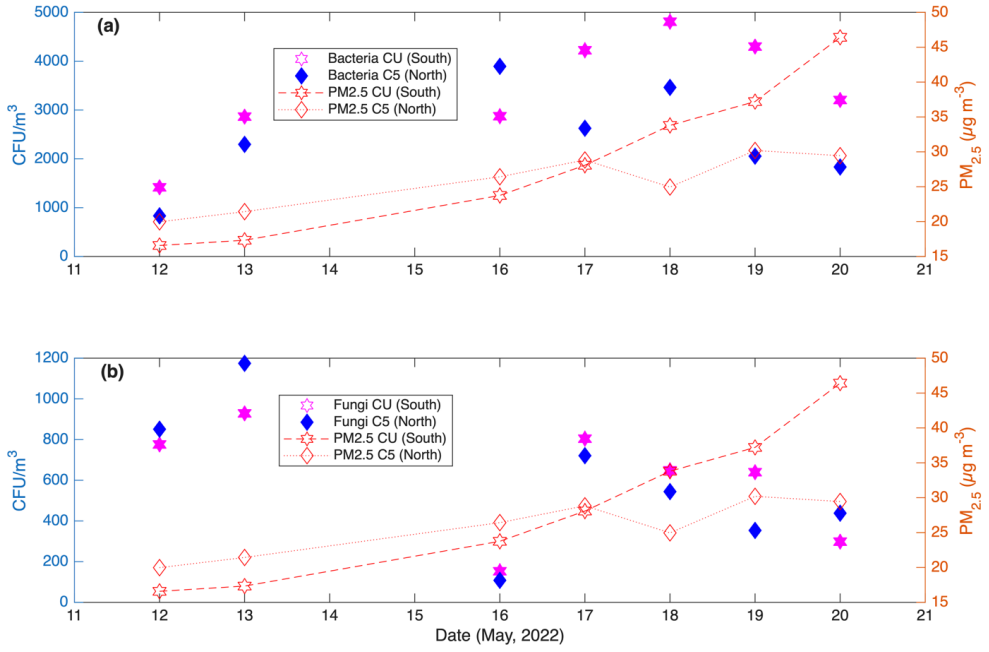

Figure 8. Time series of the concentration (CFU/m^3) of total mesophilic **a)** bacteria and **b)** fungi measured in the northern (C5, blue) and southern (CU, magenta) sites. As comparison reference, orange markers represent the $PM_{2.5}$ average concentration (µg m^{-3}) in both sites.

A total of 21 bacterial species and eight fungal genera were identified between both sampling sites (Tables S5 and S6). Although bioparticles were clearly present at both sites, it is doubtful that they played a key role in the ice nucleating abilities of the collected urban particles as the warmest average T_0 was (-17.33 ± 3.45) °C. This is very different from the T_0 values reported for bioaerosols, typically above -10 °C (Hoose et al., 2010; Knopf et al., 2011; Wex et al., 2015; Kunert et al., 2019). Although the northern site showed positive correlations between fungi concentration with T_{50}, INP Conc. (-20 °C), and INP Conc. (-25 °C) (Fig. 6), the low T_0 and T_{50} measured values, in comparison to other biological INPs, indicate that the identified culturable microorganisms did not play a primary role in the measured ice nucleating abilities of the MCMA particles.

Melchum et al. (2023) showed that among the 64 analyzed species, the most efficient INP was the *Cupriavidus pauculus* bacteria, with T_0 and T_{50} temperatures of -11.8 °C and -17.3 °C, respectively. Therefore, as demonstrated by Melchum et al. (2023) and previously by Schnell and Vali (1976), tropical biological particles appear to be inefficient INPs.

https://doi.org/10.5194/egusphere-2025-6106
Preprint. Discussion started: 9 January 2026

The variations in bacterial and fungal concentration between the northern and southern sites were evaluated by the cross-correlations shown in Tables S7 and S8. As expected, not all bacteria and fungi found at the northern site are present in the southern site.

4. Conclusions

This work evaluated, for the first time, simultaneous measurements of INP abilities at two sites within one of the largest megacities worldwide. Aerosol particles sampled in the southern and northern parts of the MCMA acted as INPs, via immersion freezing, at average temperatures below (-17.33 ± 3.5) °C and (-19.2 ± 1.9) °C, respectively. The average INP concentrations varied between (0.04 ± 0.04) L^{-1} and (23 ± 17) L^{-1} at temperatures between -15 °C and -30 °C. The measured INP concentrations agree with those from previous studies conducted in Mexico City (Mexico) and Beijing (China). Although earlier studies have shown that particle size plays a role in the ice nucleating abilities of Arctic, urban, marine, biomass burning, and mineral dust particles (e.g., Mason et al., 2016; Córdoba et al, 2020), the present results showed that the ice nucleating abilities of complex urban particles from the MCMA are not strongly size-dependent (see Fig. S4 and Fig. 5).

The INP activity of the MCMA urban particles correlated with $PM_{2.5}$, S, K, and K^+, especially at the southern site, corroborating that particle composition is very important. Also, the present results, including meteorological data, clearly demonstrated the existence of microclimates within the MCMA. Local emissions and the regional transport of different particles (e.g., BB, biogenic SOA, anthropogenic SOA, mineral dust particles, and bioaerosol), are highlighted as the primary sources of urban aerosol particles along the MCMA. These results are consistent with previous studies in the MCMA that have mostly focused on aerosol chemical composition (Molina et al., 2010; Amador-Muñoz et al., 2011; Ladino et al., 2018).

Although the distance between both sampling sites is just 16 km, aerosol sources and atmospheric processes linked to particle formation and aerosol aging are quite different. Therefore, if we aim to improve the current understanding of aerosol-cloud interactions within this megacity, it is crucial to consider the different microclimates to avoid assuming that aerosol physicochemical and biological characteristics within the megacity are homogeneous. Thus, differences in the local anthropogenic activities, biogenic emissions, population density, and land use are key drivers that must be considered.

https://doi.org/10.5194/egusphere-2025-6106
Preprint. Discussion started: 9 January 2026

Although the present work provides concrete information on the role that the chemical and biological compositions play on urban aerosol particles' INP activity, additional information and further analysis are required to fully understand the relationship between aerosol particles and cloud formation, such as particle morphology, coating, and degree of aging. Furthermore, more research is needed if the present results, related to mixed-phase clouds, may also apply to cirrus clouds.

Author contributions. KV, DR, JAC, FC, and LAL performed the field measurements. Ka KV, DR, JAC, FC, SMT, and LAL analyzed the data. GBR and LAL designed the field campaigns and were responsible for funding acquisition. KV, SMT, and EN conducted the INP analysis. OR supported the field campaigns and data acquisition. HA conducted the ionic composition analysis. JM conducted the X-ray fluorescence chemical analysis. JAC, IR, LM, and ES conducted the microorganism's identification analysis. SMT and LAL wrote the paper, addressed the reviews and editing, with contributions from all coauthors.

Competing interests. At least one of authors is part of the Editorial board.

Acknowledgments. The authors thank Alison Ruiz, Maria Isabel Saavedra, Juan Carlos Pineda, and Manuel García for their invaluable help. We thank Miguel Sanchez from the Mexico City Atmospheric Monitoring System for sharing the criteria pollutants data and for his support in using their infrastructure. We also thank the RUOA and PEMBU for sharing their meteorological data. Finally, we thank the NOAA for facilitating the use of the surface maps and HYSPLIT.

Financial support. This research was financially supported by the Consejo Nacional de Humanidades, Ciencia y Tecnología (grant no. 1024827) and the Marcos Moshinsky Foundation. Sebastian Mendoza-Téllez thanks SECIHTI for his PhD fellowship.

Data availability. Data will be made available on request.

References

Aiken, A. C., Salcedo, D., Cubison, M. J., Huffman, J. A., DeCarlo, P. F., Ulbrich, I. M., Docherty, K. S., Sueper, D., Kimmel, J. R., Worsnop, D. R., Trimborn, A., Northway, M., Stone, E. A., Schauer, J. J., Volkamer, R. M., Fortner, E., de Foy, B., Wang, J., Laskin, A.,

https://doi.org/10.5194/egusphere-2025-6106
Preprint. Discussion started: 9 January 2026

Shutthanandan, V., Zheng, J., Zhang, R., Gaffney, J., Marley, N. A., Paredes-Miranda, G., Arnott, W. P., Molina, L. T., Sosa, G., and Jimenez, J. L.: Mexico City aerosol analysis during MILAGRO using high resolution aerosol mass spectrometry at the urban supersite (T0) – Part 1: Fine particle composition and organic source apportionment, Atmos. Chem. Phys., https://doi.org/10.5194/acp-9-6633-2009, 2009.

Aldape, F., Flores M., J., Diaz, R. V., Morales, J. R., Cahill, T. A., and Saravia, L.: Seasonal study of the composition of atmospheric aerosols in Mexico City, Int. J. PIXE, 01, 355–371, https://doi.org/10.1142/S012908359100024X, 1991.

Amador-Muñoz, O., Villalobos-Pietrini, R., Miranda, J., and Vera-Avila, L. E.: Organic compounds of PM2.5 in Mexico Valley: Spatial and temporal patterns, behavior and sources, Sci. Total Environ., 409, 1453–1465, https://doi.org/10.1016/j.scitotenv.2010.11.026, 2011.

Amador-Muñoz, O., Bazán-Torija, S., Villa-Ferreira, S. A., Villalobos-Pietrini, R., Bravo-Cabrera, J. L., Munive-Colín, Z., Hernández-Mena, L., Saldarriaga-Noreña, H., and Murillo-Tovar, M. A.: Opposing seasonal trends for polycyclic aromatic hydrocarbons and PM10: Health risk and sources in southwest Mexico City, Atmos. Res., 122, 199–212, https://doi.org/10.1016/j.atmosres.2012.10.003, 2013.

Amador-Muñoz, O., Misztal, P. K., Weber, R., Worton, D. R., Zhang, H., Drozd, G., and Goldstein, A. H.: Sensitive detection of *n* -alkanes using a mixed ionization mode proton-transfer-reaction mass spectrometer, Atmos. Meas. Tech., 9, 5315–5329, https://doi.org/10.5194/amt-9-5315-2016, 2016.

Behzadi, F., Wasti, A., Haque Rahat, S., Tracy, J. N., and Ray, P. A.: Analysis of the climate change signal in Mexico City given disagreeing data sources and scattered projections, J. Hydrol.: Reg. Stud., 27, 100662, https://doi.org/10.1016/j.ejrh.2019.100662, 2020.

Bi, K., McMeeking, G. R., Ding, D. P., Levin, E. J. T., DeMott, P. J., Zhao, D. L., Wang, F., Liu, Q., Tian, P., Ma, X. C., Chen, Y. B., Huang, M. Y., Zhang, H. L., Gordon, T. D., and Chen, P.: Measurements of Ice Nucleating Particles in Beijing, China, J. Geophys. Res. Atm., 124, 8065–8075, https://doi.org/10.1029/2019JD030609, 2019.

Cabrera-Segoviano, D., Pereira, D. L., Rodriguez, C., Raga, G. B., Miranda, J., Alvarez-Ospina, H., and Ladino, L. A.: Inter-annual variability of ice nucleating particles in Mexico city, Atmos. Environ., 273, 118964, https://doi.org/10.1016/j.atmosenv.2022.118964, 2022.

Carabali, G., Villanueva-Macias, J., Ladino, L. A., Álvarez-Ospina, H., Raga, G. B., Andraca-Ayala, G., Miranda, J., Grutter, M., Silva, Ma. M., and Riveros-Rosas, D.: Characterization of aerosol particles during a high pollution episode over Mexico City, Sci. Rep., 11, 22533, https://doi.org/10.1038/s41598-021-01873-4, 2021.

Castro Romero, T., Peralta, O., Prieto, C., Santiago, N., Alvarez-Ospina, H., García Martínez, R., Saavedra Rosado, I., Espinosa Fuentes, M. D. L. L., Hernández, E., Miranda, J., Gómez, V., Solís, C., Salcedo, D., Torres-Jardón, R., Martínez-Arroyo, A., Ortínez Álvarez, A., Ruíz-Suárez, G., and Ortiz, E.: Characterization of $PM_{2.5}$ during ACU15 campaign in Mexico City, Geofis. Int., 63, 1225–1238, https://doi.org/10.22201/igeof.2954436xe.2024.63.4.1745, 2024.

Chen, J., Wu, Z., Augustin-Bauditz, S., Grawe, S., Hartmann, M., Pei, X., Liu, Z., Ji, D., and Wex, H.: Ice-nucleating particle concentrations unaffected by urban air pollution in Beijing, China, Atmos. Chem. Phys., 18, 3523–3539, https://doi.org/10.5194/acp-18-3523-2018, 2018.

https://doi.org/10.5194/egusphere-2025-6106
Preprint. Discussion started: 9 January 2026

642 Chen, J., Wu, Z., Gong, X., Qiu, Y., Chen, S., Zeng, L., and Hu, M.: Anthropogenic Dust as a
643 Significant Source of Ice-Nucleating Particles in the Urban Environment, Earth's Future, 12,
644 e2023EF003738, https://doi.org/10.1029/2023EF003738, 2024.

645 Cooke, M. E., Waters, C. M., Asare, J. Y., Mirrielees, J. A., Holen, A. L., Frauenheim, M. P.,
646 Zhang, Z., Gold, A., Pratt, K. A., Surratt, J. D., Ladino, L. A., and Ault, A. P.: Atmospheric
647 Aerosol Sulfur Distribution and Speciation in Mexico City: Sulfate, Organosulfates, and
648 Isoprene-Derived Secondary Organic Aerosol from Low NO Pathways, Environ. Sci. Technol.
649 Air, 1, 1037–1052, https://doi.org/10.1021/acsestair.4c00048, 2024.

650 Córdoba, F., Ramírez-Romero, C., Cabrera, D., Raga, G. B., Miranda, J., Alvarez-Ospina, H.,
651 Rosas, D., Figueroa, B., Kim, J. S., Yakobi-Hancock, J., Amador, T., Gutierrez, W., García,
652 M., Bertram, A. K., Baumgardner, D., and Ladino, L. A.: Measurement report: Ice nucleating
653 abilities of biomass burning, African dust, and sea spray aerosol particles over the Yucatán
654 Peninsula, Atmos. Chem. Phys., 21, 4453–4470, https://doi.org/10.5194/acp-21-4453-2021,
655 2021.

656 Cziczo, D. J., Froyd, K. D., Gallavardin, S. J., Moehler, O., Benz, S., Saathoff, H., and Murphy,
657 D. M.: Deactivation of ice nuclei due to atmospherically relevant surface coatings, Environ.
658 Res. Lett., 4, 044013, https://doi.org/10.1088/1748-9326/4/4/044013, 2009.

659 Doran, J. C., Arnott, W. P., Barnard, J. C., Cary, R., Coulter, R., Fast, J. D., Kassianov, E. I.,
660 Kleinman, L., Laulainen, N. S., Martin, T., Paredes-Miranda, G., Pekour, M. S., Shaw, W. J.,
661 Smith, D. F., and Springston, S. R.: The T1-T2 study: evolution of aerosol properties downwind
662 of Mexico City, Atmos. Chem. Phys. Discuss., 6 (6), 12967-12999.,
663 https://doi.org/10.5194/acp-7-1585-2007, 2007.

664 Draxler, R.R., R., G. D.: HYSPLIT (HYbrid Single-Particle Lagrangian Integrated Trajectory)
665 Model, 2010.

666 Edgerton, S. A., Bian, X., Doran, J. C., Fast, J. D., Hubbe, J. M., Malone, E. L., Shaw, W. J.,
667 Whiteman, C. D., Zhong, S., Arriaga, J. L., Ortiz, E., Ruiz, M., Sosa, G., Vega, E., Limon, T.,
668 Guzman, F., Archuleta, J., Bossert, J. E., Elliot, S. M., Lee, J. T., McNair, L. A., Chow, J. C.,
669 Watson, J. G., Coulter, R. L., Doskey, P. V., Gaffney, J. S., Marley, N. A., Neff, W., and Petty,
670 R.: Particulate Air Pollution in Mexico City: A Collaborative Research Project, J. Air Waste
671 Manage. Assoc., 49, 1221–1229, https://doi.org/10.1080/10473289.1999.10463915, 1999.

672 Espinosa, A., Miranda, J., and Pineda, J.C: Uncertainty evaluation in correlated quantities:
673 application to elemental analysis of atmospheric aerosols, Rev. Mex. Fís., 56 (1), 134–140,
674 2010.

675 Espinosa, A. A., Reyes-Herrera, J., Miranda, J., Mercado, F., Veytia, M. A., Cuautle, M., and
676 Cruz, J. I.: Development of an X-ray fluorescence spectrometer for environmental science
677 applications, Instrum Sci. Technol., 40, 603–617,
678 https://doi.org/10.1080/10739149.2012.693560, 2012.

679 Gimeno, L., Sorí, R., Vázquez, M., Stojanovic, M., Algarra, I., Eiras-Barca, J., Gimeno-Sotelo,
680 L., and Nieto, R.: Extreme precipitation events, WIREs Water, 9, e1611,
681 https://doi.org/10.1002/wat2.1611, 2022.

682 Hallquist, M., Wenger, J. C., Baltensperger, U., Rudich, Y., Simpson, D., Claeys, M., Dommen,
683 J., Donahue, N. M., George, C., Goldstein, A. H., Hamilton, J. F., Herrmann, H., Hoffmann,

https://doi.org/10.5194/egusphere-2025-6106
Preprint. Discussion started: 9 January 2026

T., Iinuma, Y., Jang, M., Jenkin, M. E., Jimenez, J. L., Kiendler-Scharr, A., Maenhaut, W., McFiggans, G., Mentel, T. F., Monod, A., Prevot, A. S. H., Seinfeld, J. H., Surratt, J. D., Szmigielski, R., and Wildt, J.: The formation, properties and impact of secondary organic aerosol: current and emerging issues, Atmos. Chem. Phys., https://doi.org/10.5194/acp-9-5155-2009, 2009.

Hasenkopf, C. A., Veghte, D. P., Schill, G. P., Lodoysamba, S., Freedman, M. A., and Tolbert, M. A.: Ice nucleation, shape, and composition of aerosol particles in one of the most polluted cities in the world: Ulaanbaatar, Mongolia, Atmos. Environ., 139, 222–229, https://doi.org/10.1016/j.atmosenv.2016.05.037, 2016.

Hernández-López, A. E., Miranda Martín Del Campo, J., Mugica-Álvarez, V., Hernández-Valle, B. L., Mejía-Ponce, L. V., Pineda-Santamaría, J. C., Reynoso-Cruces, S., Mendoza-Flores, J. A., and Rozanes-Valenzuela, D.: A study of $PM_{2.5}$ elemental composition in southwest Mexico City and development of receptor models with positive matrix factorization, RICA, https://doi.org/10.20937/RICA.54066, 2020.

Hernández-López, A. E., Santos-Medina, G. L., Morton-Bermea, O., Hernández-Álvarez, E., Villalobos-Pietrini, R., and Amador-Muñoz, O.: Chemical speciation of organic compounds and elemental compositions of $PM_{2.5}$ in Mexico City: Spatial-seasonal distribution, emission sources, and formation processes, Atmos. Res., 292, 106868, https://doi.org/10.1016/j.atmosres.2023.106868, 2023.

Hoose, C. and Möhler, O.: Heterogeneous ice nucleation on atmospheric aerosols: a review of results from laboratory experiments, Atmos. Chem. Phys., 12, 9817–9854, https://doi.org/10.5194/acp-12-9817-2012, 2012.

Hoose, C., Kristjánsson, J. E., and Burrows, S. M.: How important is biological ice nucleation in clouds on a global scale?, Environ. Res. Lett., 5, 024009, https://doi.org/10.1088/1748-9326/5/2/024009, 2010.

Houze, R. A.: Cloud dynamics, Second edition., Academic Press, Oxford, England, 2014.

Hurtado, L., Rodríguez, G., López, J., Castillo, J. E., Molina, L., Zavala, M., and Quintana, P. J. E.: Characterization of atmospheric bioaerosols at 9 sites in Tijuana, Mexico, Atmos. Environ., 96, 430–436, https://doi.org/10.1016/j.atmosenv.2014.07.018, 2014.

Población: https://www.inegi.org.mx/temas/estructura/, last access: 10 October 2025.

Jahl, L. G., Brubaker, T. A., Polen, M. J., Jahn, L. G., Cain, K. P., Bowers, B. B., Fahy, W. D., Graves, S., and Sullivan, R. C.: Atmospheric aging enhances the ice nucleation ability of biomass-burning aerosol, Sci. Adv., 7, https://doi.org/10.1126/sciadv.abd3440, 2021.

Jahn, L. G., Polen, M. J., Jahl, L. G., Brubaker, T. A., Somers, J., and Sullivan, R. C.: Biomass combustion produces ice-active minerals in biomass-burning aerosol and bottom ash, Proc. Natl. Acad. Sci. U.S.A., 117, 21928–21937, https://doi.org/10.1073/pnas.1922128117, 2020.

Jáuregui, E.: El clima de la Ciudad de México, 1. ed., Instituto de Geografía, UNAM : Plaza y Valdés Editores, México, D.F, 131 pp., 2000.

https://doi.org/10.5194/egusphere-2025-6106
Preprint. Discussion started: 9 January 2026

Kanji, Z. A., Ladino, L. A., Wex, H., Boose, Y., Burkert-Kohn, M., Cziczo, D. J., and Krämer, M.: Overview of Ice Nucleating Particles, Meteorol. Monogr., 58, 1.1-1.33, https://doi.org/10.1175/AMSMONOGRAPHS-D-16-0006.1, 2017.

Knopf, D. A., Wang, B., Laskin, A., Moffet, R. C., and Gilles, M. K.: Heterogeneous nucleation of ice on anthropogenic organic particles collected in Mexico City, Geophys. Res. Lett., 37, 2010GL043362, https://doi.org/10.1029/2010GL043362, 2010.

Knopf, D. A., Alpert, P. A., Wang, B., and Aller, J. Y.: Stimulation of ice nucleation by marine diatoms, Nature Geosci., 4, 88–90, https://doi.org/10.1038/ngeo1037, 2011.

Kunert, A. T., Pöhlker, M. L., Tang, K., Krevert, C. S., Wieder, C., Speth, K. R., Hanson, L. E., Morris, C. E., Schmale Iii, D. G., Pöschl, U., and Fröhlich-Nowoisky, J.: Macromolecular fungal ice nuclei in *Fusarium* : effects of physical and chemical processing, Biogeosciences, 16, 4647–4659, https://doi.org/10.5194/bg-16-4647-2019, 2019.

Ladino, L. A., Raga, G. B., and Baumgardner, D.: On particle-bound polycyclic aromatic hydrocarbons (PPAH) and links to gaseous emissions in Mexico City, Atmos. Environ., 194, 31–40, https://doi.org/10.1016/j.atmosenv.2018.09.022, 2018.

Lezama, J. L. and Vargas, V. I.: Las fuerzas rectoras de la contaminación del aire en la Ciudad de México, MIT Integrated Program on Urban, Regional and Global Air Pollution Report NO.8. Cambridge, MA, 2000.

Li, M., Qi, J., Zhang, H., Huang, S., Li, L., and Gao, D.: Concentration and size distribution of bioaerosols in an outdoor environment in the Qingdao coastal region, Science of The Total Environment, 409, 3812–3819, https://doi.org/10.1016/j.scitotenv.2011.06.001, 2011.

Mason, R. H., Chou, C., McCluskey, C. S., Levin, E. J. T., Schiller, C. L., Hill, T. C. J., Huffman, J. A., DeMott, P. J., and Bertram, A. K.: The micro-orifice uniform deposit impactor–droplet freezing technique (MOUDI-DFT) for measuring concentrations of ice nucleating particles as a function of size: improvements and initial validation, Atmos. Meas. Tech., 8, 2449–2462, https://doi.org/10.5194/amt-8-2449-2015, 2015.

Mason, R. H., Si, M., Chou, C., Irish, V. E., Dickie, R., Elizondo, P., Wong, R., Brintnell, M., Elsasser, M., Lassar, W. M., Pierce, K. M., Leaitch, W. R., MacDonald, A. M., Platt, A., Toom-Sauntry, D., Sarda-Estève, R., Schiller, C. L., Suski, K. J., Hill, T. C. J., Abbatt, J. P. D., Huffman, J. A., DeMott, P. J., and Bertram, A. K.: Size-resolved measurements of ice-nucleating particles at six locations in North America and one in Europe, Atmos. Chem. Phys., 16, 1637–1651, https://doi.org/10.5194/acp-16-1637-2016, 2016.

Melchum, A., Córdoba, F., Salinas, E., Martínez, L., Campos, G., Rosas, I., Garcia-Mendoza, E., Olivos-Ortiz, A., Raga, G. B., Pizano, B., Silva, Ma. M., and Ladino, L. A.: Maritime and continental microorganisms collected in Mexico: An investigation of their ice-nucleating abilities, Atmos. Res., 293, 106893, https://doi.org/10.1016/j.atmosres.2023.106893, 2023.

Molina, H., Yang, Y., Ruch, T., Kim, J.-W., Mortensen, P., Otto, T., Nalli, A., Tang, Q.-Q., Lane, M. D., Chaerkady, R., and Pandey, A.: Temporal Profiling of the Adipocyte Proteome during Differentiation Using a Five-Plex SILAC Based Strategy, J. Proteome Res., 8, 48–58, https://doi.org/10.1021/pr800650r, 2009.

https://doi.org/10.5194/egusphere-2025-6106
Preprint. Discussion started: 9 January 2026

Molina, L. T., Madronich, S., Gaffney, J. S., Apel, E., De Foy, B., Fast, J., Ferrare, R., Herndon, S., Jimenez, J. L., Lamb, B., Osornio-Vargas, A. R., Russell, P., Schauer, J. J., Stevens, P. S., Volkamer, R., and Zavala, M.: An overview of the MILAGRO 2006 Campaign: Mexico City emissions and their transport and transformation, Atmos. Chem. Phys., 10, 8697–8760, https://doi.org/10.5194/acp-10-8697-2010, 2010.

Molina, M. J. and Molina, L. T.: Megacities and Atmospheric Pollution, J. Air Waste Manage. Assoc., 54, 644–680, https://doi.org/10.1080/10473289.2004.10470936, 2004.

Moreno, T., Querol, X., Pey, J., Minguillón, M. C., Pérez, N., Alastuey, A., Bernabé, R. M., Blanco, S., Cárdenas, B., Eichinger, W., Salcido, A., and Gibbons, W.: Spatial and temporal variations in inhalable CuZnPb aerosols within the Mexico City pollution plume, J. Environ. Monit., 10, 370, https://doi.org/10.1039/b716507b, 2008.

Mülmenstädt, J., Sourdeval, O., Delanoë, J., and Quaas, J.: Frequency of occurrence of rain from liquid-, mixed-, and ice-phase clouds derived from A-Train satellite retrievals, Geophys. Res. Lett., 42, 6502–6509, https://doi.org/10.1002/2015GL064604, 2015.

Pereira, D. L., Silva, Ma. M., García, R., Raga, G. B., Alvarez-Ospina, H., Carabali, G., Rosas, I., Martinez, L., Salinas, E., Hidalgo-Bonilla, S., and Ladino, L. A.: Characterization of ice nucleating particles in rainwater, cloud water, and aerosol samples at two different tropical latitudes, Atmos. Res., 250, 105356, https://doi.org/10.1016/j.atmosres.2020.105356, 2021.

Pinto, D. M., Blande, J. D., Souza, S. R., Nerg, A.-M., and Holopainen, J. K.: Plant Volatile Organic Compounds (VOCs) in Ozone (O3) Polluted Atmospheres: The Ecological Effects, J. Chem. Ecol., 36, 22–34, https://doi.org/10.1007/s10886-009-9732-3, 2010.

Prenni, A. J., DeMott, P. J., Sullivan, A. P., Sullivan, R. C., Kreidenweis, S. M., and Rogers, D. C.: Biomass burning as a potential source for atmospheric ice nuclei: Western wildfires and prescribed burns, Geophys. Res. Lett., 39, https://doi.org/10.1029/2012gl051915, 2012.

Querol, X., Pey, J., Minguillón, M. C., Pérez, N., Alastuey, A., Viana, M., Moreno, T., Bernabé, R. M., Blanco, S., Cárdenas, B., Vega, E., Sosa, G., Escalona, S., Ruiz, H., and Artíñano, B.: PM speciation and sources in Mexico during the MILAGRO-2006 Campaign, Atmos. Chem. Phys., 8, 111–128, https://doi.org/10.5194/acp-8-111-2008, 2008.

Querol, X., Tobías, A., Pérez, N., Karanasiou, A., Amato, F., Stafoggia, M., Pérez García-Pando, C., Ginoux, P., Forastiere, F., Gumy, S., Mudu, P., and Alastuey, A.: Monitoring the impact of desert dust outbreaks for air quality for health studies, Environ. Int., 130, 104867, https://doi.org/10.1016/j.envint.2019.05.061, 2019.

Raga, G. B., Ladino, L. A., Baumgardner, D., Ramirez-Romero, C., Córdoba, F., Alvarez-Ospina, H., Rosas, D., Amador, T., Miranda, J., Rosas, I., Jaramillo, A., Yakobi-Hancock, J., Kim, J. S., Martínez, L., Salinas, E., and Figueroa, B.: ADABBOY: African Dust And Biomass Burning Over Yucatan, B. Am. Meteor. Soc., 102, E1543–E1556, https://doi.org/10.1175/BAMS-D-20-0172.1, 2021.

Riojas-Rodríguez, H., Álamo-Hernández, U., Texcalac-Sangrador, J. L., and Romieu, I.: Health impact assessment of decreases in PM10 and ozone concentrations in the Mexico City Metropolitan Area. A basis for a new air quality management program, SPM, 56, 579, https://doi.org/10.21149/spm.v56i6.7384, 2014.

https://doi.org/10.5194/egusphere-2025-6106
Preprint. Discussion started: 9 January 2026

Ríos, B. and Raga, G. B.: Spatio-temporal distribution of burned areas by ecoregions in Mexico and Central America, Int. J. Remote Sens., 39, 949–970, https://doi.org/10.1080/01431161.2017.1392641, 2018.

Rodríguez-Gómez, C.: Variabilidad de los núcleos de glaciación en la capa límite y la tropósfera libre en Altzomoni, y su influencia en la formación de nubes mixtas, Universidad Nacional Autónoma de México, México, CDMX, 128 pp., 2021.

Rodriguez-Gomez, C., Ramirez-Romero, C., Cordoba, F., Raga, G. B., Salinas, E., Martinez, L., Rosas, I., Quintana, E. T., Maldonado, L. A., Rosas, D., Amador, T., Alvarez, H., and Ladino, L. A.: Characterization of culturable airborne microorganisms in the Yucatan Peninsula, Atmos. Environ., 223, 117183, https://doi.org/10.1016/j.atmosenv.2019.117183, 2020.

Rogers, R. R. and Yau, M. K.: A short course in cloud physics, Third edition., Butterworth-Heinemann, Burlington, Massachusetts, 1 pp., 1996.

Russy-Velandia, L., Ramírez, O., Barrera, J., Mendoza-Téllez, S., Álvarez, H., Patiño, M. C., and Ladino, L. A.: Approach to culturable bioaerosols and their environmental drivers at a border site in the northwestern Amazon, Atmos. Environ.: X, 27, 100362, https://doi.org/10.1016/j.aeaoa.2025.100362, 2025.

Schnell, R. C. and Vali, G.: Biogenic Ice Nuclei: Part I. Terrestrial and Marine Sources, J. Atmos. Sci., 33, 1554–1564, https://doi.org/10.1175/1520-0469(1976)033%253C1554:BINPIT%253E2.0.CO;2, 1976.

Tabari, H.: Climate change impact on flood and extreme precipitation increases with water availability, Sci. Rep., 10, 13768, https://doi.org/10.1038/s41598-020-70816-2, 2020.

Vali, G.: Ice Nucleation — a review, in: Nucleation and Atmospheric Aerosols 1996, Elsevier, 271–279, https://doi.org/10.1016/B978-008042030-1/50066-4, 1996.

Vega, E., Reyes, E., Ruiz, H., García, J., Sánchez, G., Martínez-Villa, G., González, U., Chow, J. C., and Watson, J. G.: Analysis of $PM_{2.5}$ and PM_{10} in the Atmosphere of Mexico City during 2000-2002, J. Air Waste Manage. Assoc., 54, 786–798, https://doi.org/10.1080/10473289.2004.10470952, 2004.

Wang, B., Lambe, A. T., Massoli, P., Onasch, T. B., Davidovits, P., Worsnop, D. R., and Knopf, D. A.: The deposition ice nucleation and immersion freezing potential of amorphous secondary organic aerosol: Pathways for ice and mixed-phase cloud formation, J. Geophys. Res., 117, 2012JD018063, https://doi.org/10.1029/2012JD018063, 2012.

Wei, M., Xu, C., Xu, X., Zhu, C., Li, J., and Lv, G.: Size distribution of bioaerosols from biomass burning emissions: Characteristics of bacterial and fungal communities in submicron (PM1.0) and fine (PM2.5) particles, Ecotoxicol. Environ. Saf., 171, 37–46, https://doi.org/10.1016/j.ecoenv.2018.12.026, 2019.

Wex, H., Augustin-Bauditz, S., Boose, Y., Budke, C., Curtius, J., Diehl, K., Dreyer, A., Frank, F., Hartmann, S., Hiranuma, N., Jantsch, E., Kanji, Z. A., Kiselev, A., Koop, T., Möhler, O., Niedermeier, D., Nillius, B., Rösch, M., Rose, D., Schmidt, C., Steinke, I., and Stratmann, F.: Intercomparing different devices for the investigation of ice nucleating particles using Snomax®

https://doi.org/10.5194/egusphere-2025-6106
Preprint. Discussion started: 9 January 2026

as test substance, Atmos. Chem. Phys., 15, 1463–1485, https://doi.org/10.5194/acp-15-1463-2015, 2015.

Zhao, B., Wang, Y., Gu, Y., Liou, K.-N., Jiang, J. H., Fan, J., Liu, X., Huang, L., and Yung, Y. L.: Ice nucleation by aerosols from anthropogenic pollution, Nat. Geosci., 12, 602–607, https://doi.org/10.1038/s41561-019-0389-4, 2019.